Autosomal recessive *GJA1* (Cx43) gene mutations cause oculodentodigital dysplasia by distinct mechanisms

Tao Huang[1], Qing Shao[1], Andrew MacDonald[2], Li Xin[2], Robert Lorentz[1], Donglin Bai[2] and Dale W. Laird[1,2,*]

[1]Department of Anatomy and Cell Biology, University of Western Ontario, London, ON N6A-5C1, Canada
[2]Department of Physiology and Pharmacology, University of Western Ontario, London, ON N6A-5C1, Canada
*Author for correspondence (Dale.Laird@schulich.uwo.ca)

Accepted 27 March 2013
Journal of Cell Science 126, 2857–2866

doi: 10.1242/jcs.123315

Summary

Oculodentodigital dysplasia (ODDD) is mainly an autosomal dominant human disease caused by mutations in the *GJA1* gene, which encodes the gap junction protein connexin43 (Cx43). Surprisingly, there have been two autosomal recessive mutations reported that cause ODDD: a single amino acid substitution (R76H) and a premature truncation mutation (R33X). When expressed in either gap junctional intercellular communication (GJIC)-deficient HeLa cells or Cx43-expressing NRK cells, the R76H mutant trafficked to the plasma membrane to form gap junction-like plaques, whereas the R33X mutant remained diffusely localized throughout the cell, including the nucleus. As expected, the R33X mutant failed to form functional channels. In the case of the R76H mutant, dye transfer studies in HeLa cells and electrical conductance analysis in GJIC-deficient N2a cells revealed that this mutant could form functional gap junction channels, albeit with reduced macroscopic and single channel conductance. Alexa 350 dye transfer studies further revealed that the R76H mutant had no detectable negative effect on the function of co-expressed Cx26, Cx32, Cx37 or Cx40, whereas the R33X mutant exhibited significant dominant or trans-dominant effects on Cx43 and Cx40 as manifested by a reduction in wild-type connexin gap junction plaques. Taken together, our results suggest that the trans-dominant effect of R33X together with its complete inability to form a functional channel may explain why patients harboring this autosomal recessive R33X mutant exhibit greater disease burden than patients harboring the R76H mutant.

Key words: Cx43, Gap junctions, Oculodentodigital dysplasia, *GJA1*

Introduction

Gap junctions are specialized membrane channels that allow for the transfer of small molecules, ions, metabolites and second messengers between the cytoplasms of two connected cells (Alexander and Goldberg, 2003). Gap junctions are produced as the result of an oligomerization of six connexin (Cx) proteins, forming a connexon, which is delivered to the plasma membrane (Goodenough et al., 1996; Laird, 2006). A connexon can exist either as a singular unit within the plasma membrane, known as a hemichannel, or dock with a connexon from an opposing cell forming a gap junction channel which proceeds to cluster with other channels to form gap junction plaques frequently consisting of hundreds of channels (Goodenough and Paul, 2003). There are 21 members in the human connexin family, all of which are predicted to share a similar membrane topology consisting of four transmembrane domains, two extracellular loops, an intracellular loop with the amino and carboxyl termini exposed to the cytoplasm (Laird, 2006; Laird and Revel, 1990; Söhl and Willecke, 2004).

Connexins are temporally and spatially regulated in human physiology, and many cell types are known to express one or more connexin isoforms (Laird, 2006). As a result, various connexin hexamers can exist resulting in channel selectivity unique to its connexin constituents (Laird, 2006). Connexons and gap junction channels composed of one connexin are termed homomeric and homotypic, respectively; whereas those composed of two or more distinct connexins are termed heteromeric and heterotypic; respectively (Goodenough et al., 1996). As a result of the ubiquitous expression of connexins and a resulting immense network of gap junctional intercellular communication (GJIC), it is not at all surprising to find that connexin mutations or changes in GJIC lead to many human pathologies (Laird, 2008; Pfenniger et al., 2011).

Mutations in the gene encoding the almost ubiquitously expressed connexin, Cx43, results in the predominantly autosomal dominant disease called oculodentodigital dysplasia (ODDD) (Paznekas et al., 2003). ODDD is characterized by several common clinical phenotypes such as syndactyly and camptodactyly of the digits, microdontia, enamel loss, ophthalmic defects and craniofacial abnormalities (Paznekas et al., 2003; Paznekas et al., 2009). To date, over 65 known mutations, spanning the Cx43 gene coding sequence, have been linked to ODDD (Laird, 2006; Laird, 2008; Paznekas et al., 2003; Paznekas et al., 2009). The majority of the autosomal dominant mutations examined to date have been shown to reduce channel function and act as dominant-negatives on the function of co-expressed wild-type Cx43 (Flenniken et al., 2005; Gong et al., 2007; Gong et al., 2006; McLachlan et al., 2005). However, recent clinical presentations and genetic screens have revealed two (R76H and R33X) autosomal recessive mutations linked to

Journal of Cell Science

ODDD (Paznekas et al., 2009; Pizzuti et al., 2004; Richardson et al., 2006). Interestingly, recessive Cx43 mutations provide a unique platform to study the function of Cx43 throughout various tissues and organs of the human body. Previous studies employing systemic Cx43 knockout mice revealed that Cx43 is required for normal heart development and that the loss of Cx43 is lethal at birth (Reaume et al., 1995). In humans, the R33X autosomal recessive mutant, consisting of only a 32 amino acid segment representing the N-terminus and a partial fragment of the first transmembrane domain of Cx43 is not expected to form gap junction channels, suggesting that these patients are essentially equivalent to a Cx43 knockout. Unlike knockout mice, patients homozygous for the R33X mutant do survive past birth, although they display very severe clinical symptoms of ODDD including small deep-set eyes and other ophthalmological defects, extensive syndactyly, many dental abnormalities and other defects that severely compromise life expectancy (Richardson et al., 2006). However, the patients harboring the autosomal recessive R76H mutant appeared to share similarities to the autosomal dominant ODDD patients but also carry characteristics of Hallermann-Streiff syndrome that result in small stature, hypotrichosis and many teeth and skeletal abnormalities (Pizzuti et al., 2004). This raises the notion that the R76H mutant may have residual gap junction channel function, although this has yet to be tested. Nevertheless, it is intriguing that different Cx43 mutants cause different pleiotropic disease symptoms.

In the current study we assessed the localization and function of the R76H and R33X autosomal recessive Cx43 mutants. We found that the R76H mutant can form functional gap junction channels with reduced coupling, whereas the R33X mutant failed to traffic properly and form functional gap junction channels. We further found that the R76H mutant had no trans-dominant effects on the function of co-expressed Cx40, Cx37, Cx26 or Cx32. However, the R33X mutant exhibited dominant and trans-dominant-negative effects on co-expressed Cx43, Cx37 and Cx40. These results suggest that the reason why patients harboring the autosomal recessive R33X mutant possess greater and more far reaching morbidities than R76H patients may be rooted in the fact that the R33X mutant has no innate channel forming ability and may further inhibit connexin family members that are frequently co-expressed with Cx43 in a wide variety of tissues and organs.

Results

The R76H mutant localized to sites of cell to cell apposition in HeLa and NRK cells

Cx43-negative HeLa cells were transiently transfected with cDNA constructs encoding the autosomal recessive R76H and R33X Cx43 mutants. Immunofluorescence revealed that both the untagged R76H and GFP-tagged R76H mutant assembled gap junction-like plaques at cell interfaces (Fig. 1A,B, arrowheads), like wild-type Cx43 (Fig. 1A,B, arrowheads). However, both the FLAG and GFP-tagged R33X mutant failed to form any plaques and exhibited a homogenous cytoplasm and nuclear localization profile in HeLa cells (Fig. 1A,B). Similarly, the R76H mutant formed gap junction-like plaques at sites of cell-to-cell appositions in Cx43-positive NRK cells, whereas the R33X

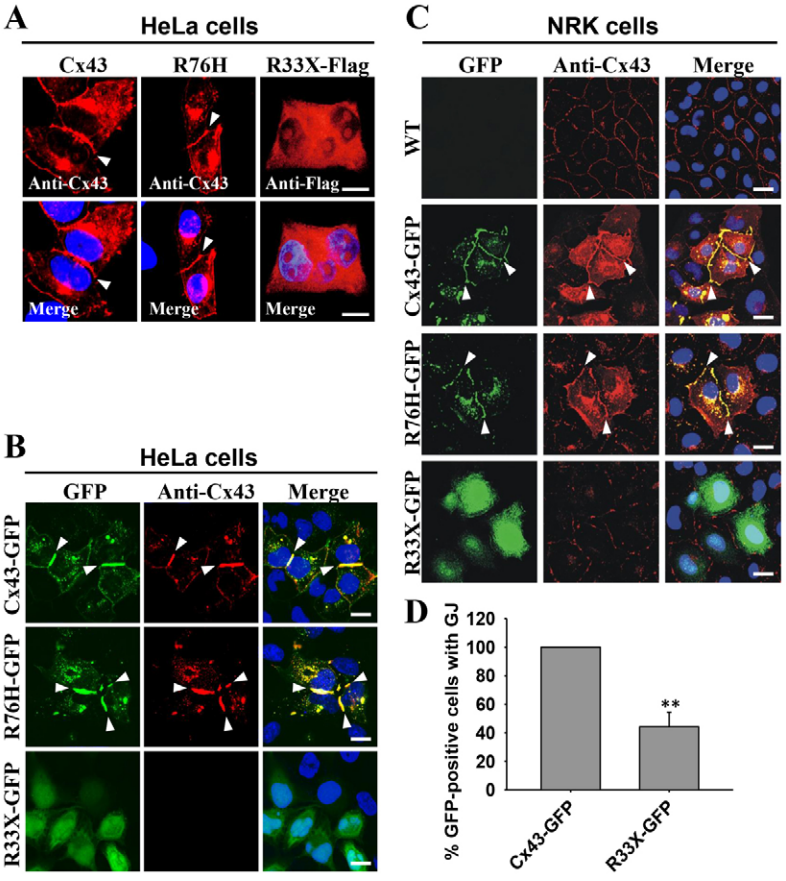

Fig. 1. Localization of Cx43 mutants. (**A**) HeLa cells were engineered to express Cx43, the R76H mutant or the FLAG-tagged R33X mutant prior to immunolabeling for Cx43 or FLAG and Hoechst staining of the nuclei. (**B**) HeLa cells were further constructed to express GFP-tagged Cx43, the R76H mutant or the R33X mutant prior to immunolabeling for Cx43 and Hoechst staining. (**C**) Cx43-positive NRK cells were engineered to express GFP-tagged (green) Cx43, the R76H mutant or the R33X mutant prior to immunolabeling for Cx43 (red). Arrowheads reveal that gap junction plaques formed from Cx43 and the R76H mutant. WT, wild type. (**D**) The percentage of cells expressing Cx43-GFP or R33X-GFP that exhibited immunolabeled Cx43 gap junction (GJ) plaques was quantified. $^{**}P<0.01$. Scale bars: 10 μm.

mutant exhibited a diffused intracellular distribution that included entering the nucleus (Fig. 1C). Furthermore, in NRK cells expressing the R33X mutant, there was a reduction in Cx43 gap junctions (Fig. 1D). These results indicated that the R76H mutant localizes to gap junction-like plaque structures, whereas the R33X mutant failed to even reach the cell surface but acted to reduce the number of Cx43 gap junctions.

Functional status of Cx43 mutants

To determine if the autosomal recessive mutants (R76H and R33X) can form functional channels, mutant expressing HeLa cells were microinjected with Lucifer yellow (443 Da) or Alexa 350 (350 Da) and the incidents of dye transfer were assessed. Whereas the R33X mutant failed to allow either dye to pass, the R76H mutant was equally well at passing Alexa 350 as wild-type Cx43 and about 40% as efficient in transferring Lucifer yellow when again directly compared to wild-type Cx43 (Fig. 2A,B). Thus, whereas the R76H mutant was capable of forming a functional channel, the R33X mutant was functionally dead. Interestingly, only the R33X mutant inhibited the function of Cx43 when both were co-expressed in HeLa cells and this was irrespective of whether the mutant was tagged with RFP or GFP (Fig. 2C). When cells co-expressing R33X-GFP and Cx43 were immunoprecipitated for endogenous Cx43, the R33X mutant was pulled down (Fig. 2D). If the R33X mutant was acting to inhibit Cx43 channel function by a physical interaction we predicted that the extent of channel inhibition would escalate with increased levels of mutant expression. To test this hypothesis, we expressed the RFP-tagged R33X mutant in calcein AM loaded Cx43-positive NRK cells and selectively examined fluorescence recovery after photobleaching (FRAP) in high and low mutant expressing cells. FRAP analysis revealed that cells expressing high levels of the R33X mutant exhibited significantly less fluorescence recovery compared to low mutant expressing cells and untransfected control cells (Fig. 3). Collectively, these findings would suggest that the R33X mutant likely interacts with Cx43 to inhibit the function of wild-type channels.

The R76H mutant forms channels with reduced single channel conductance

Given the fact that dye transfer studies showed that the R76H mutant can form functional gap junction channels in HeLa cells, we proceeded to assess their channel forming ability in GJIC-deficient N2a cells through double patch-clamp recordings. As shown in Fig. 4A, the average macroscopic junctional conductance (g_j) of R76H-GFP channels was 1.9 nS ($n=14$),

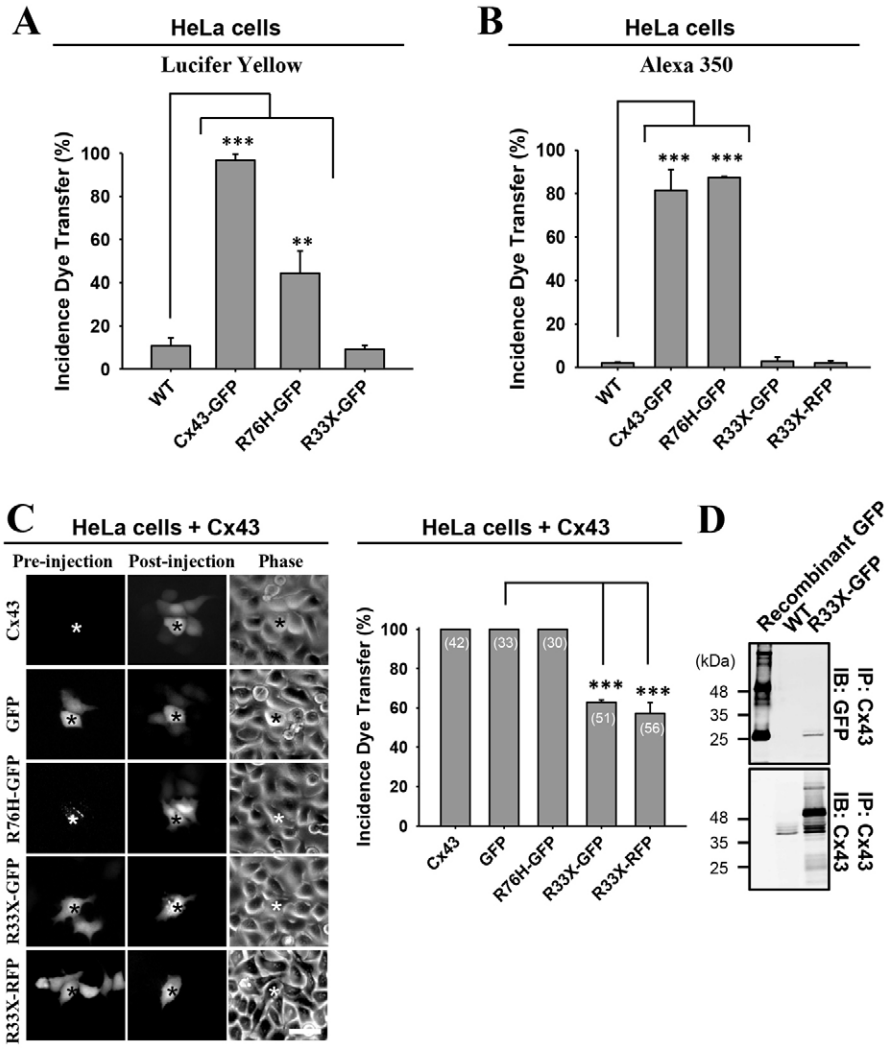

Fig. 2. The R76H mutant is functional while the non-functional R33X mutant inhibits co-expressed Cx43. (**A**) HeLa cells or HeLa cells engineered to express Cx43-GFP, R76H-GFP or R33X-GFP mutants were microinjected with Lucifer yellow, and the incidences of dye transfer were quantified. $^{**}P<0.01$; $^{***}P<0.001$. (**B**) Likewise, HeLa cells expressing Cx43-GFP, R76H-GFP, R33X-GFP or R33X-RFP were microinjected with Alexa 350, and the incidences of dye transfer were quantified. $^{***}P<0.001$. Note that cells expressing Cx43 or the R76H mutant were capable of dye transfer. (**C**) HeLa cells expressing Cx43 were transfected with constructs encoding GFP, R76H-GFP, R33X-GFP or R33X-RFP prior to the microinjection of Alexa 350. Images of the pre-injected cells represent the GFP or RFP fluorescence. Post-injection images represent the fluorescence from Alexa 350. Microinjected cells (denoted by asterisks) were imaged prior to dye microinjection, after dye injection and under phase-contrast microscopy, and the incidences of GFP or mutant expressing cells passing dye to surrounding Cx43 expressing cells was quantified (right). Note that the expression of the R33X mutant impaired dye transfer. $^{***}P<0.001$. Numbers in parentheses denote the number of cells injected with dye. Scale bar: 20 μm. (**D**) HeLa cells or HeLa cells co-expressing Cx43 and the R33X-GFP mutant were immunoprecipitated (IP) for Cx43, and immunoprecipitates were subjected to immunoblotting (IB) for GFP or Cx43. Recombinant GFP was used as a control for anti-GFP antibody labeling. The Ig heavy chain and Cx43 were detected with the anti-Cx43 antibody. Note that the R33X mutant was immunoprecipitated with full length Cx43, suggesting that they interacted.

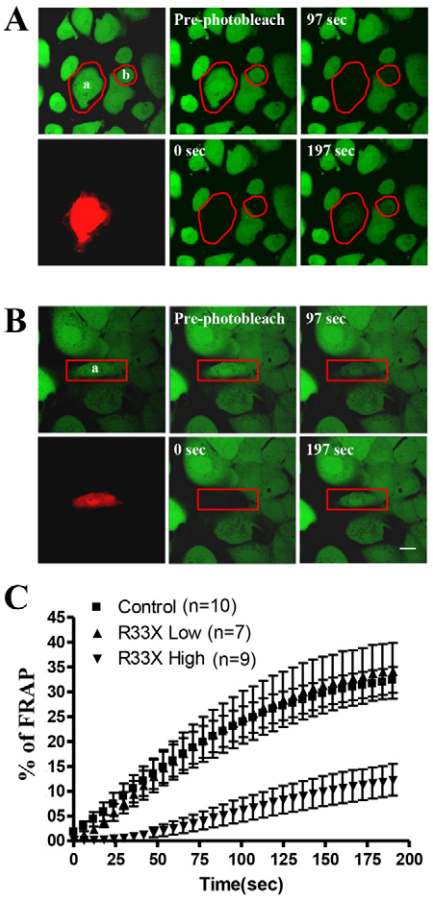

Fig. 3. High levels of the R33X mutant impaired GJIC. NRK cells expressing R33X-RFP were preloaded with calcein and subjected to fluorescence recovery after photobleaching (FRAP). Cells expressing high levels of R33X mutant (a) or no mutant (b) (panel **A**), or low levels of the R33X mutant (a in panel **B**), were photobleached and calcein recovering into the photobleached cell was tracked (**C**). Green fluorescence represents the calcein, and red fluorescence denotes the R33X mutant. The photobleached areas are outlined in red in (A) and defined within a red rectangular shape in (B) where a small corner of a contacting cell instantly refilled with green dye. Scale bar:10 μm.

which is significantly lower than that of wild-type Cx43 gap junction channels (g_j=18.5 nS, n=27, P<0.01). To further determine if the lower g_j in R76H-GFP channels was caused by a reduction of the single gap junction channel conductance, we performed single gap junction channel analysis. Fig. 4B illustrates representative single R76H-GFP gap junction channel currents recorded under V_j pulses of 40 and 80 mV. The analysis of 4 cell pairs yielded channels with an average unitary conductance (γ_j) of 41 pS, which is substantially smaller than that of Cx43 channels (120 pS) (Elenes et al., 1999) and GFP-tagged Cx43 channels (110 pS) (Bukauskas et al., 2001; Bukauskas et al., 2000). These results demonstrated that the R76H mutant forms functional gap junction channels in N2a cells with a substantially reduced unitary conductance.

Cx43 mutants have no trans-dominant effects on co-expressed Cx26 and Cx32

Since the R33X and R76H mutants are known to result in considerably different levels of disease burden (Paznekas et al., 2009; Pizzuti et al., 2004; Richardson et al., 2006), we reasoned that this may be mechanistically linked to their differential abilities to impair the function of connexins co-expressed in the same cell type. Since Cx26 and Cx32 do not form heterotypic or heteromeric channels with Cx43 and are rarely co-expressed in the same cells as Cx43, we further reasoned that the mutants would not act as trans-dominants on their function. To test this hypothesis, we co-expressed the mutants in HeLa cells stably expressing Cx26 (Fig. 5A,B) or Cx32 (Fig. 5C,D). Immunofluorescence and western blotting revealed that the host HeLa cells rigorously expressed Cx26 or Cx32 and the co-expression of the mutants did not change the expression level of either Cx26 or Cx32 (Fig. 5A–D). Subsequent Alexa 350 dye transfer studies further revealed that neither the R76H nor R33X mutants acted as a trans-dominant and inhibited dye transfer (Fig. 6A–D). Thus, as one might predict, the mutants appeared to not interact or impair the function of either Cx26 or Cx32.

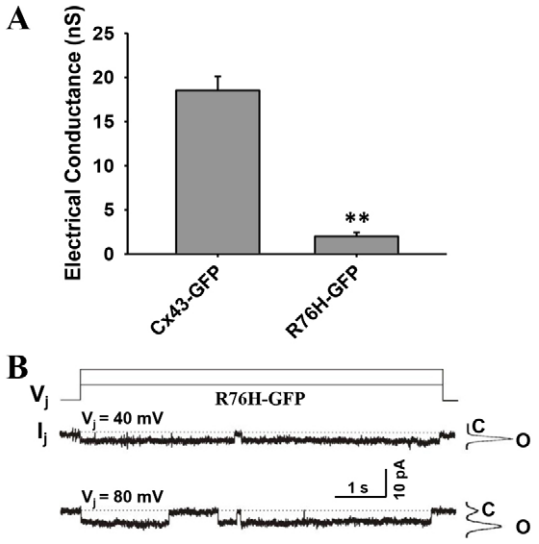

Fig. 4. Macroscopic and unitary channel conductance of the R76H mutant. (**A**) N2a cells were engineered to express either Cx43-GFP or R76H-GFP. Dual patch-clamp whole cell recording was used to assess the macroscopic electrical conductance (g_j). R76H mutant-expressing cell pairs showed a substantially lower level of electrical conductance compared with that obtained from cell pairs expressing Cx43 (**P<0.01). (**B**) The mutant expressing cell pairs were further assessed for single channel conductance. Representative single R76H-GFP gap junction channel currents were recorded under V_j pulses of 40 mV and 80 mV. The analysis of four cell pairs yielded an average γ_j of 41 pS.

The R33X mutant had a trans-dominant effect on Cx40 and Cx37

In situ, Cx43 is frequently co-expressed with Cx37 and/or Cx40 raising the possibility that these connexins may be affected by the co-expression of the disease-linked Cx43 mutants. To test this hypothesis, HeLa cells expressing Cx40 (Fig. 7A–C) or Cx37 (Fig. 7D) were further transfected to express the R33X or R76H mutants. Cells co-expressing Cx40 and the R33X mutant (Fig. 7A) exhibited less Cx40 gap junction plaques (Fig. 7B). Western blotting revealed a robust expression of the mutants with wild-type Cx40 (Fig. 7C) and Cx37 (Fig. 7D), and the levels of the wild-type connexins were unaffected by the co-expression of

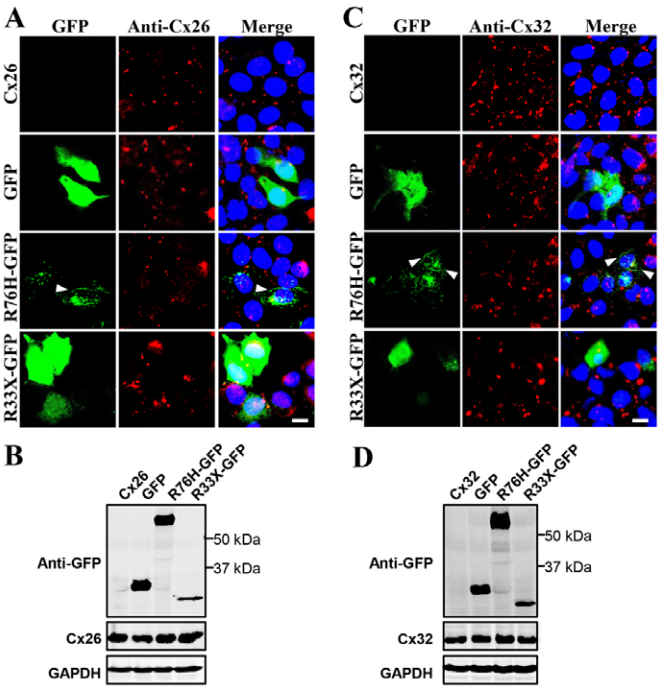

Fig. 5. Co-expression of Cx43 mutants with Cx26 or Cx43. HeLa cells expressing Cx26 or Cx32 were engineered to co-express GFP, R76H-GFP or R33X-GFP and immunolabeled for Cx26 (**A**) or Cx32 (**C**) followed by Hoechst staining (blue). Western blots revealed that Cx26 (**B**) and Cx32 (**D**) were expressed at high levels in cells that co-expressed the mutants as denoted by immunoblotting for GFP (B,D). GAPDH was used as a loading control (B,D). Scale bars: 20 µm.

either the R76H or R33X mutants. Dye transfer studies revealed that both the R76H mutant and wild-type Cx43 increased coupling in HeLa cells over the levels achieved in HeLa cells expressing Cx40 (Fig. 8A,B) or Cx37 (Fig. 8C,D) alone. Conversely, the R33X mutant significantly reduced the incidents of dye coupling when co-expressed with either Cx40 or Cx37 (Fig. 8). These findings suggest that the R33X mutant was acting as a trans-dominant inhibitor of GJIC. However, co-immunoprecipitation attempts to determine if the R33X mutant physically interacted with Cx40 or Cx37 failed (data not shown).

Discussion

Oculodentodigital dysplasia (ODDD) was classified as a developmental disease many decades ago but it was not until 2003 that it was definitively linked to mutations in the *GJA1* gene that encodes Cx43 (Paznekas et al., 2003). This seminal discovery linked Cx43-based GJIC to abnormalities in tissue and organ development that typically affects the eyes, teeth, digits and skeleton (Paznekas et al., 2003; Paznekas et al., 2009). However, in addition to these developmental abnormalities, many patients exhibit other deformities that include hyperkeratosis, urinary incontinence and CNS disorders (Paznekas et al., 2003; Paznekas et al., 2009). The broad scope of disease tissues found in some, but not all, ODDD patients may not be of great surprise, as we know that Cx43 is expressed in over 35 distinct human tissues (Laird, 2006). Originally, ODDD was thought to be exclusively a disease linked to autosomal dominant mutations which would allow for the possibility that the allele harboring the wild-type gene could suffice to provide sufficient Cx43-based GJIC and allow patients to maintain

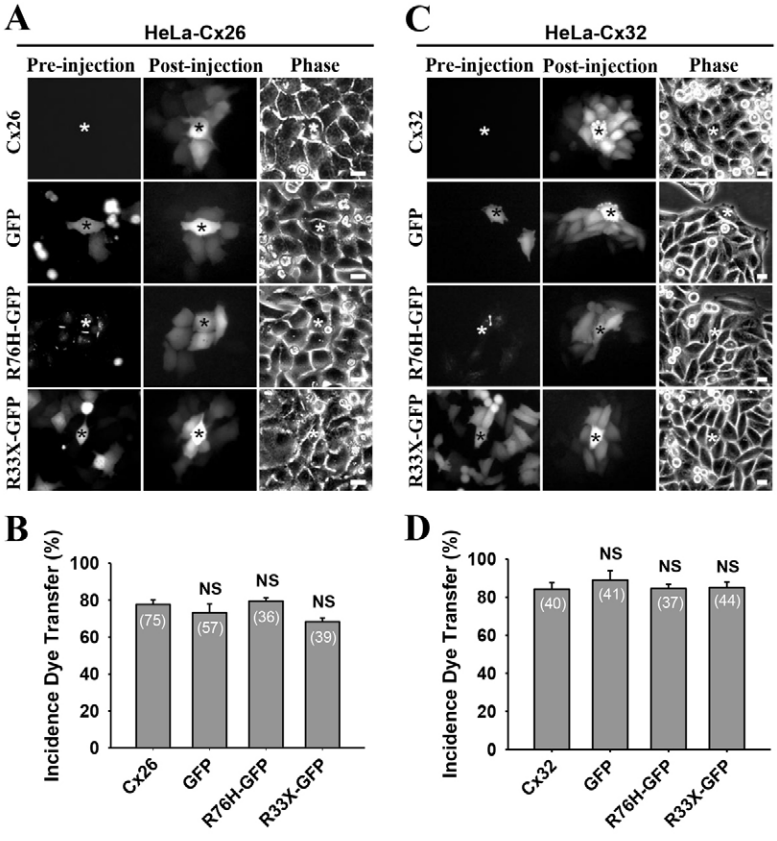

Fig. 6. Cx43 mutants have no trans-dominant effects on Cx26 and Cx32 function. HeLa cells expressing Cx26 (**A**,**B**) or Cx32 (**C**,**D**) and co-expressing GFP, R76H-GFP or R33X-GFP mutants were microinjected with Alexa 350, and the incidences of dye transfer were quantified (B,D). Numbers in parentheses represent the number of microinjected cells (B,D). Images of the pre-injected cells represent GFP fluorescence. Images of post-injected cells represent the fluorescence from Alexa 350. Microinjected cells (denoted by asterisks) were imaged prior to dye microinjection, after dye injection and under phase-contrast microscopy and the incidences of GFP or mutant expressing cells passing dye to surrounding connexin expressing cells was quantified. NS, not significant. Scale bars: 20 µm.

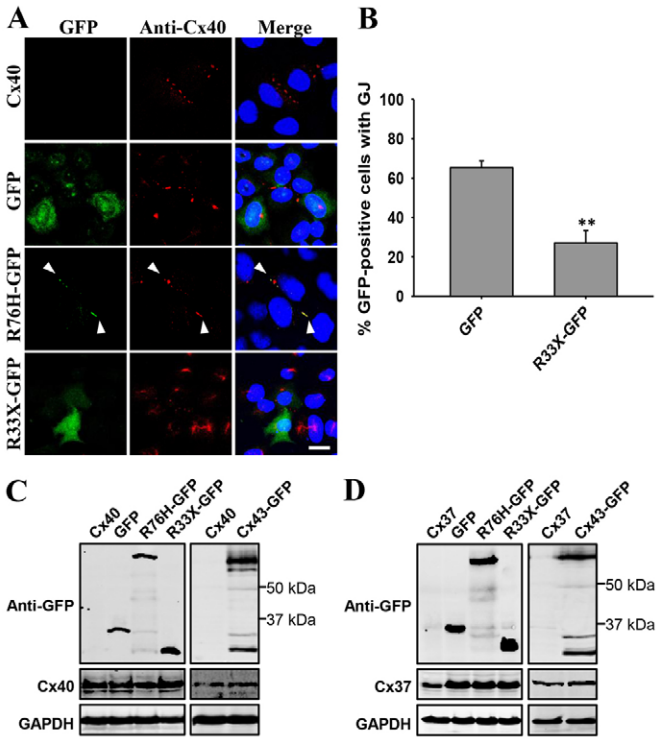

Fig. 7. Co-expression of Cx43 mutants with Cx37 or Cx40. (**A**) HeLa cells expressing Cx40 were engineered to co-express GFP, R76H-GFP or R33X-GFP and immunolabeled for Cx40. (**B**) The percentage of cells containing immunolabeled Cx40 gap junction (GJ) plaques was quantified in cells expressing GFP or the R33X-GFP mutant. ** $P<0.01$. (**C**,**D**) Western blots for connexins revealed that Cx40 (C) and Cx37 (D) were expressed at high levels in cells that co-expressed the GFP-tagged mutants, GFP or Cx43-GFP as denoted by immunoblotting for GFP. GAPDH was used as a loading control. Scale bar: 20 µm.

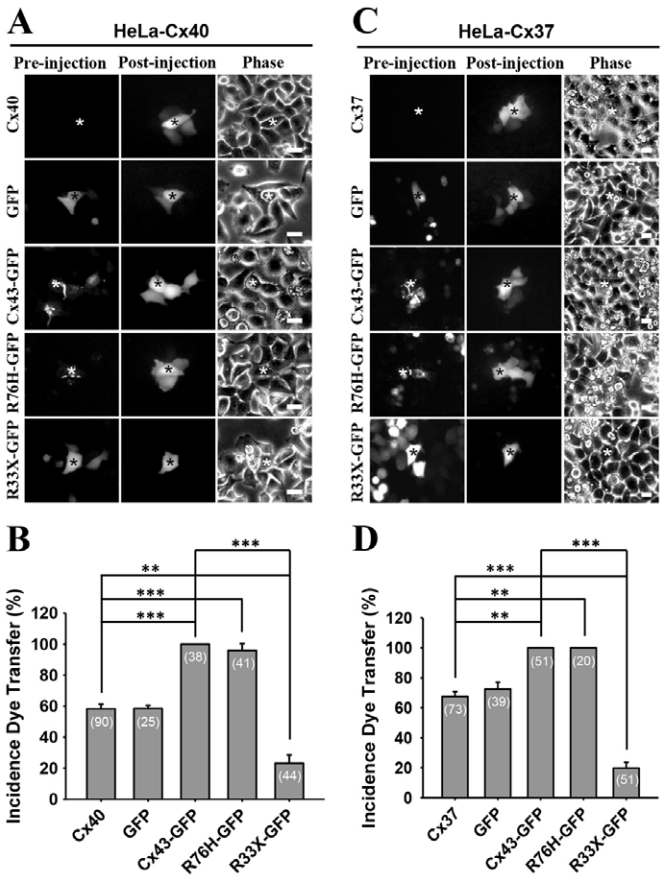

Fig. 8. The R33X mutant had a trans-dominant effect on Cx40 and Cx37. HeLa cells expressing Cx40 (**A**,**B**) or Cx37 (**C**,**D**) and co-expressing, Cx43-GFP, GFP or the mutants were microinjected with Alexa 350 and the incidences of dye transfer were quantified (B,D). Microinjected cells (denoted by asterisks) were imaged prior to dye microinjection, after dye injection and under phase-contrast microscopy and the incidences of GFP or mutant expressing cells passing dye to surrounding connexin expressing cells was quantified. Note that the expression of Cx43 or the R76H mutant increased dye transfer, whereas the R33X mutant inhibited dye transfer. Scale bars: 20 µm. Numbers in parentheses represent the number of microinjected cells (B,D). ** $P<0.01$; *** $P<0.001$.

essential organ function as seems to be the case in the heart where Cx43 is abundant (Gros and Jongsma, 1996). Many of these autosomal dominant mutants have been categorized by us and others as loss-of-function mutants, gain-of-hemichannel function mutants or dominant-negative mutants on co-expressed wild-type Cx43 (Churko et al., 2011a; Churko et al., 2012; Churko et al., 2010; Churko et al., 2011b; Dobrowolski et al., 2009; Dobrowolski et al., 2008; Dobrowolski et al., 2007; Flenniken et al., 2005; Gong et al., 2007; Gong et al., 2006; Lai et al., 2006; Langlois et al., 2007; Lorentz et al., 2012; Manias et al., 2008; McLachlan et al., 2005; McLachlan et al., 2008; Musa et al., 2009; Shao et al., 2012; Shibayama et al., 2005; Stewart et al., 2013; Toth et al., 2010). However, our understanding of the characteristics of Cx43 mutants became more complicated when two autosomal recessive mutations were identified that encoded a severely truncated Cx43 (R33X) (Richardson et al., 2006) and an arginine to a histidine (R76H) substitution within the domain predicted to be at the extreme region of the 1st extracellular loop (Pizzuti et al., 2004). In the present study, we examined the unique properties of these disease-linked mutants and how the mutations translate to disease with variable severity.

Two young patients have been documented to harbor the recessive R33X mutant and exhibit severe developmental defects typically associated with ODDD (Richardson et al., 2006). In addition, to classical ODDD one of these patients exhibited characteristics of severe motor and speech defects, indicative of stark CNS defects, and was considered to have a life threatening condition (Richardson et al., 2006). The affected sister of the proband also had severe ODDD but exhibited no delay in motor skill development, albeit she was not followed for any substantial period (Richardson et al., 2006). Interestingly the parents of these patients who were heterozygous for the R33X mutation appeared to be clinically unaffected (Richardson et al., 2006), suggesting that a 50% complement of wild-type Cx43 expression was sufficient to preserve normal development, not unlike what is observed in the $Cx43^{+/-}$ heterozygous knockout mice (Reaume et al., 1995). In another instance of homozygous inheritance of ODDD, a patient harbored a R76H mutant where again the heterozygous carrying parents were found to be clinically normal (Pizzuti et al., 2004). Interestingly this ODDD patient shared clinical symptoms with a related developmental disorder known as Hallermann-Streiff syndrome which is characterized by having a small stature, hypotrichosis, congenital cataracts, pointed nose and other teeth and skeletal deformities (Pizzuti et al., 2004).

When the arginine residue at position 76 was substituted with a serine, patients acquire autosomal dominant ODDD (Pizzuti et al., 2004) which indicates that the nature of the substitution is of critical importance when linking to dominant or recessive inheritance of Cx43-linked disease. The R76 residue is highly conserved among the connexin family members and known to cause hearing loss and palmoplantar keratoderma when mutated in Cx26 (Paznekas et al., 2009) suggesting this residue is likely of critical importance for the function of at least a subset of connexins.

When the R76H mutant was expressed in GJIC-deficient HeLa cells it trafficked to the cell surface and assembled into gap junction channels that were found to be functionally compromised and exhibited a unitary conduction of 41 pS which is well below the expected 110–120 pS reported for untagged and GFP-tagged wild-type Cx43 (Bukauskas et al., 2001; Bukauskas et al., 2000; Elenes et al., 1999). Consistently, channels formed from the R76H mutant were also capable of passing dye. Although many ODDD linked mutants are dominant to co-expressed wild-type Cx43, we found that the R76H mutant exhibited no dominant-negative properties on either the trafficking of wild-type Cx43 to the cell surface and plaque formation or on the overall level of dye transfer between mutant expressing cells. Thus, the heterozygous parents of the homozygous R76H patient would be expected to be utilizing the full complement of Cx43 encoded on the normal allele as well as the residual channel activity provided by the R76H mutant itself. Collectively, this >60% based Cx43-GJIC appears to be sufficient for the parents to be clinically normal. In addition, the fact that the R76H mutant exhibited no evidence of trans-dominant-negative properties on other co-expressed connexins such as Cx37 or Cx40 further suggests that these ODDD patients may have normal levels of non-Cx43-based GJIC. Remarkably, the residual channel forming ability of the R76H mutant that ranges from 15% (electrophysiology assessment) to >40% (Alexa 350 and Lucifer yellow dye transfer assessment) is sufficient to allow patients to survive, although they suffer from ODDD. Given that the dye transfer studies performed here are based on a simple “yes” or “no” as to whether any dye was observed to pass from the mutant expressing cell to adjoining cells, we suggest the 15% normal level of gap junction electrical conductance is probably a more accurate assessment of the functional capacity of the mutant.

When the R33X mutant was expressed in GJIC-deficient HeLa cells, it failed to traffic to the cell surface, even when tagged with a small epitope tag (FLAG), and was found throughout the cell cytoplasm and the nucleus. Not surprisingly, this mutant failed to form any functional gap junction channels, strongly suggesting that R33X patients survive in the absence of any Cx43-based GJIC. Interestingly, the R33X mutant had a modest dominant-negative effect on co-expressed Cx43 reducing the incidence of dye coupling by ~40% in HeLa cells stably engineered to express Cx43 and a similar reduction of ~50% in Cx43-based gap junction plaques seen in Cx43-positive NRK cells that co-expressed the mutant. The dominant-negative effect of the R33X mutant appeared to be rooted in the ability of the mutant to physically interact with wild-type Cx43 possibly causing misfolding and reduced trafficking of Cx43 to the cell surface where gap junction assembly is completed. However, it is important to note that we have no evidence that the molecular ratio of mutant to endogenous Cx43 is at a ratio of 1:1 which would be the case in parents of R33X harboring ODDD patients. The fact that NRK cells expressing low levels of the R33X mutant failed to alter the functional status of endogenous Cx43 might explain why heterozygous R33X mutant carriers (parents of R33X autosomal recessive patients) do not exhibit clinically detectable ODDD (Richardson et al., 2006). Conversely, our data showed that when the R33X mutant is highly expressed, there was a clear reduction in the functional status of co-expressed Cx43.

Since the N-terminus of Cx43 is thought to be responsible for governing the oligomerization process (Lagree et al., 2003), we reasoned that the 32 amino acid fragment of Cx43 translated in R33X patients may be sufficient to interact and possible interfere with the function of other related members of the 21 member connexin family. Consistent with this notion, the R33X mutant exhibited trans-dominant-negative effects on cells engineered to co-express Cx37 and Cx40, whereas it exhibited no GJIC effects on cells that expressed Cx26 and Cx32, suggesting that the inhibitory effect is not non-specific. Although Cx43 is frequently co-expressed with Cx37 and/or Cx40 in cells of the heart, skin, ovaries, testis, blood vessels, cornea and other tissues (Gemel et al., 2012; Gros and Jongsma, 1996; Laux-Fenton et al., 2003), it is rarely co-expressed in the same cells as Cx26 or Cx32 (Söhl and Willecke, 2004). Furthermore, Cx43 is not thought to be capable of co-oligomerization with either Cx26 or Cx32, whereas it has been documented to form heteromeric channels with both Cx37 (Brink et al., 1997) and Cx40 (He et al., 1999). We propose that the N-terminal fragment of Cx43 generated in patients harboring the R33X mutant may interact with Cx37 and Cx40 inhibiting their function and broadening the scope of affected tissues and the overall severity of the disease. However, we could not directly show that the R33X mutant could interact with Cx37 or Cx40 raising concerns as to whether this is the mechanism of action. We suspect that this mechanism could still be the case but the interaction of the mutant with either Cx37 or Cx40 is transient and unstable resulting in a misfolding of the connexin, prematurely targeting it for degradation rather than passage through the secretory pathway and gap junction assembly. The fact that there was an observed reduction in gap junctions composed of Cx40 in cells expressing the mutant would support the notion that the mutant is at least altering the total number of Cx40 molecules available for gap junction assembly.

In summary, this is the first characterization of the only two known autosomal recessive Cx43 mutants linked to ODDD. From our studies, patients that harbor the R33X mutant are deemed to be surviving with no Cx43-based GJIC, and we predict that other closely related connexin family members may also be compromised resulting in the most extreme and severe form of clinically reported ODDD to date. Interestingly the heterozygous parents of R33X patients have no clinical symptoms of ODDD suggesting that sufficient functional Cx43 remains available for proper organ development and function. On the other hand, we discovered that the R76H mutant retains the ability to make functional channels, albeit the channels are functionally compromised. In this case, ODDD is not as severe as in the R33X patients but it transcends into exhibiting additional symptoms commonly associated with Hallermann-Streiff syndrome, whereas the related R76S mutant causes strictly ODDD symptoms (Pizzuti et al., 2004). We propose that R76H patients will suffer from fewer morbidities than R33X patients due to the residual channel activity retained by the mutant and the

lack of any evidence that the mutant cross-talks and inhibits the channel forming ability of other co-expressed connexin family members. Finally, we have elucidated two clearly distinct mechanisms of how Cx43 mutants are linked to disease, and based on these discoveries, we provide a better understanding as to why ODDD patients may have greater or less disease burden.

Material and Methods

Cell culture and reagents

All media, sera, and culture reagents were obtained from Invitrogen. N2a (mouse neuroblastoma), normal rat kidney (NRK) and HeLa (human cervical carcinoma) cells were purchased from American Type Culture Collection. Cells were cultured at 37℃ and 5% CO_2 in Dulbecco's Modified Essential Medium (DMEM), 4.5 g/l D-glucose supplemented with 10% fetal bovine serum, 100 μg/ml penicillin, 100 μg/ml streptomycin and 2 mM L-glutamine. HeLa cells were stably engineered to express Cx43, Cx37 or Cx26 by retroviral infection as we have described previously (Mao et al., 2000; Qin et al., 2002) or transiently engineered to express Cx40. HeLa cells stably expressing Cx32 were generously provided by Dr Michael Koval (Emory University, GA).

Engineering of mutant Cx43 cDNAs

The vector encoding human Cx43-GFP was previously described (McLachlan et al., 2008; Roscoe et al., 2005). The human cDNA construct encoding the GFP-tagged R76H mutant was purchased from Norclone Biotech Industries (London, ON). The R33X-GFP encoding construct was engineered by using the forward primer of human Cx43 (5′-GAC GAC AAG CTT ATG GGT GAC TGG AGC G) to introduce the *Hin*dIII site and the reverse primer (5′-TCG GAT CCG CGA AAA TGA AAA GTA CT) to introduce the *Bam*HI site. The PCR products were digested with *Hin*dIII/*Bam*HI and cloned into the *Hin*dIII/*Bam*HI-cut pEGFP-N1 (Clontech) vector. DNA sequence analysis confirmed that the first 32 amino acids from human Cx43 was fused in-frame to the N-terminus of GFP via a seven amino acid linker. To engineer the FLAG-tagged R33X mutant, we used a reverse primer (5′-GCG CGG ATC CGA AAA TGA AAA GTA CTG) to introduce a BamH1 site and proceeded to follow the same approach as used to engineer the GFP-tagged mutant where the GFP vector was replaced with the p3×flag-CMV-14 vector (Sigma-Aldrich). Sequence analysis confirmed that the R33X mutant was fused in-frame to the FLAG epitope via a 4 amino acid linker. The pTaqRFP vector was purchased from Evrogen (Evrogen JSC, Miklukho-Maklaya 16/10, Moscow, 117420, Russia). The GFP-tagged R33X vector was digested with *Bam*HI and *Hin*dIII restriction enzymes to excise the R33X coding region prior to ligating to RFP to generate a vector encoding R33X-RFP. DNA sequencing confirmed that RFP was fused in-frame to the C-terminus of the first 32 amino acids of human Cx43 via a 7 amino acid linker sequence. As a control, a GFP encoding vector was used to engineer cells expressing free GFP. Expressed GFP resolved at a slightly higher molecular weight than recombinant GFP (data not shown) presumably due to the inclusion of amino acid components of the multiple cloning site and differences in folding characteristics upon interaction with SDS.

Immunocytochemistry

Cells were immunolabeled as previously described (Gong et al., 2007; Gong et al., 2006; Manias et al., 2008). Briefly, cells were grown on glass coverslips and fixed with 80% methanol/20% acetone at 4℃ for 15 minutes. Cells expressing Cx43 or mutant Cx43 were labeled with a 1:500 dilution of anti-Cx43 antibody (Sigma-Aldrich). All anti-Cx26, Cx32, Cx37 and Cx40 antibodies were purchased from Invitrogen and used at a 1:100 dilution. Primary antibody binding was detected using goat anti-mouse or donkey anti-rabbit antibodies conjugated to Alexa 555 (Invitrogen). Nuclei were stained with Hoechst 33342 at 10 μg/ml (Molecular Probes). Coverslips were rinsed in distilled water, mounted, and analyzed on Zeiss LSM 510 Meta confocal microscope as previously described (Qin et al., 2003; Veitch et al., 2004).

To quantify gap junction plaques in cells co-expressing connexins together with GFP, Cx43-GFP or R33X-GFP, we imaged NRK cells or HeLa cells immunolabeled for Cx43 or Cx40, respectively. Ten randomly selected images (60×60 μm) for each condition were scored for the total number of GFP-positive cells in each field and whether these same cells exhibited clear evidence (two or more disguisable plaques) of immunolabeled Cx43 or Cx40 gap junction plaques at locations of cell–cell interfaces. The percent of GFP-positive cells that were also positive for Cx43 or Cx40 gap junction plaques was plotted±s.e.m. (** $P<0.01$).

Dye transfer studies

Control cells or cells expressing GFP-tagged Cx43 or mutants were pressure microinjected with a glass pipette contain 5% Lucifer yellow or 10 mM Alexa 350 (Molecular Probes, Canada) using an Eppendorf FemtoJet automated pressure microinjector attached to a Leica DM IRE2 inverted epifluorescence microscope. Approximately, 1–2 min after microinjection, digital images were collected with a charge-coupled device camera (Hamamatsu Photonics, Japan) using OpenLab software (Improvision). For data analysis, cells were imaged initially for GFP (pre-injection images), whereas "post-injection" images reflected the presence and spread of Lucifer yellow or Alexa 350. The percentage of microinjected GFP, connexin or mutant-expressing cells that exhibited dye transfer to one or more contacting cells was quantified as a measure of dye transfer as previously described (Jordan et al., 1999; McLachlan et al., 2006).

Western blotting

Connexin and mutant expressing cells were lysed in detergent-based buffer (150 mM NaCl, 10 mM Tris-HCl, pH 7.4, 1 mM EDTA, 1 mM EGTA, 0.5% Nonidet P-40, 1% Triton X-100, 1 mM NaF, 1 mM Na_3VO_4 and proteases inhibitors). Approximately 40 μg of protein per lane was resolved on in 10% SDS-PAGE. The proteins were transferred onto nitrocellulose membranes, blocked in 5% milk at room temperature and incubated with primary antibodies overnight at 4℃. Cx43, Cx26, Cx32, Cx37, Cx40 and GFP were detected using polyclonal anti-Cx43 (1:5000; Sigma C6219), polyclonal anti-Cx26 (1:500; Invitrogen 71-0500), polyclonal anti-Cx32 (1:500; Sigma C3470), polyclonal anti-Cx37 (1:500; Invitrogen 40-4300), polyclonal anti-Cx40 (1:200; Invitrogen 36-4900) and monoclonal anti-GFP (1:1000; Chemicon MAB3580) antibody. In some cases, recombinant GFP was used as a control for anti-GFP antibody binding. The membranes were also probed for GAPDH antibody (1:10,000; Chemicon MAB374) as a control for protein loading. Immunoreactive bands were revealed following 1-hour incubation with Alexa Fluor 680 (red; 1:10,000 dilution; Invitrogen, Canada) or IRDye 800 conjugated secondary antibodies (green; 1:10,000 dilution; Rockland, Gilbertsville, PA) and visualized using the Odyssey Infrared Imaging System (Li-Cor Biosciences, Lincoln, NE).

Co-immunoprecipitation

NRK cells or cells expressing R33X-GFP were lysed in RIPA buffer (1% Triton X-100, 10 mM Tris, 150 mM NaCl, 1 mM EDTA, 1 mM EGTA, 0.5% NP-40, 1 mM NaF and 1 mM Na_3VO_4). The cellular lysates were homogenized, cleared, and immunoprecipitated by using anti-Cx43 antibodies (2 μg/reaction; Sigma C6219) at 4℃ overnight. Immune complexes were precipitated with 30 μl of pre-cleaned Protein A–Sepharose beads (in PBS) for 2 hours on the rocker at 4℃. The antibody bead complex was centrifuged at 1940 ***g***, at 4℃ for 2 minutes and supernatants were aspirated. Unbound proteins were separated from bound proteins by washing three times with 500 μl of RIPA buffer, and the bound complex was detached from the beads by boiling for 5 minutes in 30 μl of 2× Laemmli loading buffer containing β-mercaptoethanol. Samples were resolved by 10% SDS-PAGE and transferred to nitrocellulose membranes which were probed with anti-GFP and anti-Cx43 antibodies.

Patch clamp electrophysiology

N2a cells were transfected with the R76H-GFP mutant or its control, Cx43-GFP. Double whole-cell patch-clamp recordings were performed by using two Axopatch 200B amplifiers (Axon Instruments, Union City, CA). The macroscopic junctional conductance (g_j) of Cx43-GFP and R76H-GFP gap junction channels were assessed as previously described (Xin et al., 2010). To ensure accuracy of the g_j, off-line compensation was used to correct junctional voltage (V_j) errors resulting from the series resistance of each patch electrode in the g_j calculations (Musa et al., 2004). Recordings from cell pairs displaying one or two channels were used to determine the unitary current amplitudes. The γ_j was calculated by dividing the measured amplitudes of unitary current (I_j) by the V_j; $\gamma_j=I_j/V_j$. The amplitudes of I_js were either determined by direct measurements or by first plotting all-points current amplitude histograms and then fitting these histograms with Gaussian functions to determine the mean and variance of the baseline and open channel current. The junctional current signal was low-pass filtered at 1 kHz and digitized at 10 kHz, and the recorded unitary currents were digitally filtered by a low-pass Gaussian filter (200 Hz) for presentation.

Fluorescence recovery after photobleaching (FRAP)

Monolayer cultures of Cx43-positive NRK cells were transfected with R33X-RFP. After 24 hours, cells were incubated with 10 μg/ml calcein-AM (Molecular Probes) in culture medium for 10 min prior to washing twice in PBS. Live cells were imaged on a Zeiss LSM 510 META confocal microscope equipped for detecting red (RFP) and green (calcein) fluorescence. Untransfected cells or cells expressing high and low levels of the R33X-RFP mutant were selected and the green-fluorescent calcein bleached with an argon laser. "High" mutant expressing cells exhibited RFP pixel saturation throughout the entire area of the cell and "low" mutant expressing cells exhibited cell areas that were not saturated by RFP fluorescence. Images were collected before bleaching and every 6 seconds after bleaching for 198 seconds to assess the recovery of green-fluorescent calcein into the photobleached cells. In some cases there was a slight decrease in the overall brightness of the calcein fluorescent image fields due to repeated laser scanning used for image acquisition. Data was processed using LSM software and plotted as

the percent FRAP over time (±s.e.) for each photobleached cell (n=7–10) using GraphPad Prism4.

Statistics

All values are presented as mean±s.e. unless otherwise indicated. All results were analyzed using the Student's two-tailed independent sample t-test. All analyses were done by using the SigmaStat statistical software. $P<0.05$ was considered to be a statistically significant difference.

Acknowledgements

The authors thank Jamie Simek for his assistance with the confocal imaging and FRAP analysis. The authors declare no conflicts of interest.

Author contributions

T.H. performed the majority of the experiments and prepared most of the figures. Q.S. directly prepared many of the constructs, designed experiments and did the FRAP experiments. R.L. performed pilot studies on the Cx43 mutants. A.M., L.X. and D.B. performed the electrophysiological experiments. D.W.L. supervised the project and the writing of the manuscript.

Funding

This work was supported by grants from the Canadian Institute of Health Research (to D.W.L. and D.B.).

References

Alexander, D. B. and Goldberg, G. S. (2003). Transfer of biologically important molecules between cells through gap junction channels. *Curr. Med. Chem.* **10**, 2045-2058.

Brink, P. R., Cronin, K., Banach, K., Peterson, E., Westphale, E. M., Seul, K. H., Ramanan, S. V. and Beyer, E. C. (1997). Evidence for heteromeric gap junction channels formed from rat connexin43 and human connexin37. *Am. J. Physiol.* **273**, C1386-C1396.

Bukauskas, F. F., Jordan, K., Bukauskiene, A., Bennett, M. V., Lampe, P. D., Laird, D. W. and Verselis, V. K. (2000). Clustering of connexin 43-enhanced green fluorescent protein gap junction channels and functional coupling in living cells. *Proc. Natl. Acad. Sci. USA* **97**, 2556-2561.

Bukauskas, F. F., Bukauskiene, A., Bennett, M. V. and Verselis, V. K. (2001). Gating properties of gap junction channels assembled from connexin43 and connexin43 fused with green fluorescent protein. *Biophys. J.* **81**, 137-152.

Churko, J. M., Langlois, S., Pan, X., Shao, Q. and Laird, D. W. (2010). The potency of the fs260 connexin43 mutant to impair keratinocyte differentiation is distinct from other disease-linked connexin43 mutants. *Biochem. J.* **429**, 473-483.

Churko, J. M., Chan, J., Shao, Q. and Laird, D. W. (2011a). The G60S connexin43 mutant regulates hair growth and hair fiber morphology in a mouse model of human oculodentodigital dysplasia. *J. Invest. Dermatol.* **131**, 2197-2204.

Churko, J. M., Shao, Q., Gong, X. Q., Swoboda, K. J., Bai, D., Sampson, J. and Laird, D. W. (2011b). Human dermal fibroblasts derived from oculodentodigital dysplasia patients suggest that patients may have wound-healing defects. *Hum. Mutat.* **32**, 456-466.

Churko, J. M., Kelly, J. J., Macdonald, A., Lee, J., Sampson, J., Bai, D. and Laird, D. W. (2012). The G60S Cx43 mutant enhances keratinocyte proliferation and differentiation. *Exp. Derm.* **21**, 612-618.

Dobrowolski, R., Sommershof, A. and Willecke, K. (2007). Some oculodentodigital dysplasia-associated Cx43 mutations cause increased hemichannel activity in addition to deficient gap junction channels. *J. Membr. Biol.* **219**, 9-17.

Dobrowolski, R., Sasse, P., Schrickel, J. W., Watkins, M., Kim, J. S., Rackauskas, M., Troatz, C., Ghanem, A., Tiemann, K., Degen, J. et al. (2008). The conditional connexin43G138R mouse mutant represents a new model of hereditary oculodentodigital dysplasia in humans. *Hum. Mol. Genet.* **17**, 539-554.

Dobrowolski, R., Hertig, G., Lechner, H., Wörsdörfer, P., Wulf, V., Dicke, N., Eckert, D., Bauer, R., Schorle, H. and Willecke, K. (2009). Loss of connexin43-mediated gap junctional coupling in the mesenchyme of limb buds leads to altered expression of morphogens in mice. *Hum. Mol. Genet.* **18**, 2899-2911.

Elenes, S., Rubart, M. and Moreno, A. P. (1999). Junctional communication between isolated pairs of canine atrial cells is mediated by homogeneous and heterogeneous gap junction channels. *J. Cardiovasc. Electrophysiol.* **10**, 990-1004.

Flenniken, A. M., Osborne, L. R., Anderson, N., Ciliberti, N., Fleming, C., Gittens, J. E., Gong, X. Q., Kelsey, L. B., Lounsbury, C., Moreno, L. et al. (2005). A Gja1 missense mutation in a mouse model of oculodentodigital dysplasia. *Development* **132**, 4375-4386.

Gemel, J., Nelson, T. K., Burt, J. M. and Beyer, E. C. (2012). Inducible coexpression of connexin37 or connexin40 with connexin43 selectively affects intercellular molecular transfer. *J. Membr. Biol.* **245**, 231-241.

Gong, X. Q., Shao, Q., Lounsbury, C. S., Bai, D. and Laird, D. W. (2006). Functional characterization of a GJA1 frameshift mutation causing oculodentodigital dysplasia and palmoplantar keratoderma. *J. Biol. Chem.* **281**, 31801-31811.

Gong, X. Q., Shao, Q., Langlois, S., Bai, D. and Laird, D. W. (2007). Differential potency of dominant negative connexin43 mutants in oculodentodigital dysplasia. *J. Biol. Chem.* **282**, 19190-19202.

Goodenough, D. A. and Paul, D. L. (2003). Beyond the gap: functions of unpaired connexon channels. *Nat. Rev. Mol. Cell Biol.* **4**, 285-294.

Goodenough, D. A., Goliger, J. A. and Paul, D. L. (1996). Connexins, connexons, and intercellular communication. *Annu. Rev. Biochem.* **65**, 475-502.

Gros, D. B. and Jongsma, H. J. (1996). Connexins in mammalian heart function. *Bioessays* **18**, 719-730.

He, D. S., Jiang, J. X., Taffet, S. M. and Burt, J. M. (1999). Formation of heteromeric gap junction channels by connexins 40 and 43 in vascular smooth muscle cells. *Proc. Natl. Acad. Sci. USA* **96**, 6495-6500.

Jordan, K., Solan, J. L., Dominguez, M., Sia, M., Hand, A., Lampe, P. D. and Laird, D. W. (1999). Trafficking, assembly, and function of a connexin43-green fluorescent protein chimera in live mammalian cells. *Mol. Biol. Cell* **10**, 2033-2050.

Lagree, V., Brunschwig, K., Lopez, P., Gilula, N. B., Richard, G. and Falk, M. M. (2003). Specific amino-acid residues in the N-terminus and TM3 implicated in channel function and oligomerization compatibility of connexin43. *J. Cell Sci.* **116**, 3189-3201.

Lai, A., Le, D. N., Paznekas, W. A., Gifford, W. D., Jabs, E. W. and Charles, A. C. (2006). Oculodentodigital dysplasia connexin43 mutations result in non-functional connexin hemichannels and gap junctions in C6 glioma cells. *J. Cell Sci.* **119**, 532-541.

Laird, D. W. (2006). Life cycle of connexins in health and disease. *Biochem. J.* **394**, 527-543.

Laird, D. W. (2008). Closing the gap on autosomal dominant connexin-26 and connexin-43 mutants linked to human disease. *J. Biol. Chem.* **283**, 2997-3001.

Laird, D. W. and Revel, J. P. (1990). Biochemical and immunochemical analysis of the arrangement of connexin43 in rat heart gap junction membranes. *J. Cell Sci.* **97**, 109-117.

Langlois, S., Maher, A. C., Manias, J. L., Shao, Q., Kidder, G. M. and Laird, D. W. (2007). Connexin levels regulate keratinocyte differentiation in the epidermis. *J. Biol. Chem.* **282**, 30171-30180.

Laux-Fenton, W. T., Donaldson, P. J., Kistler, J. and Green, C. R. (2003). Connexin expression patterns in the rat cornea: molecular evidence for communication compartments. *Cornea* **22**, 457-464.

Lorentz, R., Shao, Q., Huang, T., Fishman, G. I. and Laird, D. W. (2012). Characterization of gap junction proteins in the bladder of Cx43 mutant mouse models of oculodentodigital dysplasia. *J. Membr. Biol.* **245**, 345-355.

Manias, J. L., Plante, I., Gong, X. Q., Shao, Q., Churko, J., Bai, D. and Laird, D. W. (2008). Fate of connexin43 in cardiac tissue harbouring a disease-linked connexin43 mutant. *Cardiovasc. Res.* **80**, 385-395.

Mao, A. J., Bechberger, J., Lidington, D., Galipeau, J., Laird, D. W. and Naus, C. C. (2000). Neuronal differentiation and growth control of neuro-2a cells after retroviral gene delivery of connexin43. *J. Biol. Chem.* **275**, 34407-34414.

McLachlan, E., Manias, J. L., Gong, X. Q., Lounsbury, C. S., Shao, Q., Bernier, S. M., Bai, D. and Laird, D. W. (2005). Functional characterization of oculodentodigital dysplasia-associated Cx43 mutants. *Cell Commun. Adhes.* **12**, 279-292.

McLachlan, E., Shao, Q., Wang, H. L., Langlois, S. and Laird, D. W. (2006). Connexins act as tumor suppressors in three-dimensional mammary cell organoids by regulating differentiation and angiogenesis. *Cancer Res.* **66**, 9886-9894.

McLachlan, E., Plante, I., Shao, Q., Tong, D., Kidder, G. M., Bernier, S. M. and Laird, D. W. (2008). ODDD-linked Cx43 mutants reduce endogenous Cx43 expression and function in osteoblasts and inhibit late stage differentiation. *J. Bone Miner. Res.* **23**, 928-938.

Musa, H., Fenn, E., Crye, M., Gemel, J., Beyer, E. C. and Veenstra, R. D. (2004). Amino terminal glutamate residues confer spermine sensitivity and affect voltage gating and channel conductance of rat connexin40 gap junctions. *J. Physiol.* **557**, 863-878.

Musa, F. U., Ratajczak, P., Sahu, J., Pentlicky, S., Fryer, A., Richard, G. and Willoughby, C. E. (2009). Ocular manifestations in oculodentodigital dysplasia resulting from a heterozygous missense mutation (L113P) in GJA1 (connexin 43). *Eye (Lond.)* **23**, 549-555.

Paznekas, W. A., Boyadjiev, S. A., Shapiro, R. E., Daniels, O., Wollnik, B., Keegan, C. E., Innis, J. W., Dinulos, M. B., Christian, C., Hannibal, M. C. et al. (2003). Connexin 43 (GJA1) mutations cause the pleiotropic phenotype of oculodentodigital dysplasia. *Am. J. Hum. Genet.* **72**, 408-418.

Paznekas, W. A., Karczeski, B., Vermeer, S., Lowry, R. B., Delatycki, M., Laurence, F., Koivisto, P. A., Van Maldergem, L., Boyadjiev, S. A., Bodurtha, J. N. et al. (2009). GJA1 mutations, variants, and connexin 43 dysfunction as it relates to the oculodentodigital dysplasia phenotype. *Hum. Mutat.* **30**, 724-733.

Pfenniger, A., Wohlwend, A. and Kwak, B. R. (2011). Mutations in connexin genes and disease. *Eur. J. Clin. Invest.* **41**, 103-116.

Pizzuti, A., Flex, E., Mingarelli, R., Salpietro, C., Zelante, L. and Dallapiccola, B. (2004). A homozygous GJA1 gene mutation causes a Hallermann-Streiff/ODDD spectrum phenotype. *Hum. Mutat.* **23**, 286.

Qin, H., Shao, Q., Curtis, H., Galipeau, J., Belliveau, D. J., Wang, T., Alaoui-Jamali, M. A. and Laird, D. W. (2002). Retroviral delivery of connexin genes to human breast tumor cells inhibits in vivo tumor growth by a mechanism that is independent of significant gap junctional intercellular communication. *J. Biol. Chem.* **277**, 29132-29138.

Qin, H., Shao, Q., Igdoura, S. A., Alaoui-Jamali, M. A. and Laird, D. W. (2003). Lysosomal and proteasomal degradation play distinct roles in the life cycle of Cx43 in gap junctional intercellular communication-deficient and -competent breast tumor cells. *J. Biol. Chem.* **278**, 30005-30014.

Reaume, A. G., de Sousa, P. A., Kulkarni, S., Langille, B. L., Zhu, D., Davies, T. C., Juneja, S. C., Kidder, G. M. and Rossant, J. (1995). Cardiac malformation in neonatal mice lacking connexin43. *Science* **267**, 1831-1834.

Richardson, R. J., Joss, S., Tomkin, S., Ahmed, M., Sheridan, E. and Dixon, M. J. (2006). A nonsense mutation in the first transmembrane domain of connexin 43 underlies autosomal recessive oculodentodigital syndrome. *J. Med. Genet.* **43**, e37.

Roscoe, W., Veitch, G. I., Gong, X. Q., Pellegrino, E., Bai, D., McLachlan, E., Shao, Q., Kidder, G. M. and Laird, D. W. (2005). Oculodentodigital dysplasia-causing connexin43 mutants are non-functional and exhibit dominant effects on wild-type connexin43. *J. Biol. Chem.* **280**, 11458-11466.

Shao, Q., Liu, Q., Lorentz, R., Gong, X. Q., Bai, D., Shaw, G. S. and Laird, D. W. (2012). Structure and functional studies of N-terminal Cx43 mutants linked to oculodentodigital dysplasia. *Mol. Biol. Cell* **23**, 3312-3321.

Shibayama, J., Paznekas, W., Seki, A., Taffet, S., Jabs, E. W., Delmar, M. and Musa, H. (2005). Functional characterization of connexin43 mutations found in patients with oculodentodigital dysplasia. *Circ. Res.* **96**, e83-e91.

Söhl, G. and Willecke, K. (2004). Gap junctions and the connexin protein family. *Cardiovasc. Res.* **62**, 228-232.

Stewart, M. K., Gong, X. Q., Barr, K. J., Bai, D., Fishman, G. I. and Laird, D. W. (2013). The severity of mammary gland developmental defects is linked to the overall functional status of Cx43 as revealed by genetically modified mice. *Biochem. J.* **449**, 401-413.

Toth, K., Shao, Q., Lorentz, R. and Laird, D. W. (2010). Decreased levels of Cx43 gap junctions result in ameloblast dysregulation and enamel hypoplasia in Gja1Jrt/+ mice. *J. Cell. Physiol.* **223**, 601-609.

Veitch, G. I., Gittens, J. E., Shao, Q., Laird, D. W. and Kidder, G. M. (2004). Selective assembly of connexin37 into heterocellular gap junctions at the oocyte/granulosa cell interface. *J. Cell Sci.* **117**, 2699-2707.

Xin, L., Gong, X. Q. and Bai, D. (2010). The role of amino terminus of mouse Cx50 in determining transjunctional voltage-dependent gating and unitary conductance. *Biophys. J.* **99**, 2077-2086.